Characterization of Rockwell Scientific LWIR HgCdTe Detector Arrays

Candice M. Bacon[a], Craig W. McMurtry[a], Judith L. Pipher[a], William J. Forrest[a], James D. Garnett[b], Donald Lee[b], and Dennis D. Edwall[b]

[a]University of Rochester, Rochester, NY, USA
[b]Rockwell Scientific Company, Camarillo, CA, USA

ABSTRACT

Future infrared space missions will undoubtedly employ passively cooled focal plane arrays (T $\sim$ 30K), as well as passively cooled telescopes. Most long-wave detector arrays (e.g. Si:As IBC) require cooling to temperatures of $\sim$ 6-8K.[1] We have been working with Rockwell Scientific Company to produce $\geq$ 10 μm cutoff HgCdTe detector arrays that, at temperatures of $\sim$ 30K, exhibit sufficiently low dark current and sufficiently high detective quantum efficiency, as well as high uniformity in these parameters, to be interesting for astronomy. Our goal is to achieve dark current below the target value of $\sim 30e^-/s$/pixel with at least 60mV of actual reverse bias across the diodes at T $\sim$ 30K. To this end, Rockwell Scientific Company has delivered the first array in a new order, for characterization in Rochester. Recent array deliveries of 10μm cutoff HgCdTe bonded to a Hawaii-1RG multiplexer utilize the smallest capacitance diode type. We present preliminary results on this latest 10 μm cutoff HgCdTe low dark current detector array.

Keywords: Long Wave InfraRed (LWIR) Detector, HgCdTe, Dark Current, Diode Characterization, Infrared Space Missions

1. INTRODUCTION

In order to realize future infrared space missions that employ passive cooling instead of active cooling, long wavelength detector arrays must be able to function at temperatures attainable by passive cooling. Future telescopes in space, with proper design, will be able to attain focal plane temperatures of, at best, 30K. Therefore we have been pursuing development of long wavelength HgCdTe detector arrays that will exhibit low dark current and relatively high quantum efficiencies at temperatures $\geq$30K.

Space background radiation levels drive dark current requirements. The zodiacal dust cloud emission is the dominant background at $\lambda < 30\mu$m. Cosmic Background Explorer (COBE) measured $< 2000e^-$/s/pixel or $30e^-$/s/pixel for 10μm or 5μm respectively at the South Ecliptic Pole, where this background is a minimum (see Figure 1). InSb and MWIR HgCdTe at 30K covers the wavelength range out to 5.3μm well. Thus for background-limited space operation, we concentrate on dark currents $< 30e^-$/s/pixel, with lower dark currents desirable.

At the 2002 Hawaii SPIE meeting (Bacon et al. 2003),[2] we reported on a long-wave 256×256 HgCdTe detector array with 9 different diode structures bonded to a NICMOS3 multiplexer and cooled to 30K. The best structures (small diodes) exhibited $\sim$ 30% of pixels with dark currents $< 100e^-$/s. Rockwell Scientific Company has delivered the first of several arrays exploiting the best diode structure determined previously, with high quality MBE[3] growth, and a 512×512 format detector array bonded to a Hawaii-1RG multiplexer, for characterization at the University of Rochester. This array has incorporated our previous research on 8μm to 10μm cutoff HgCdTe arrays, which shows that a smaller capacitance diode has lower dark current and higher yield than its larger counterparts. We report here preliminary results on this device. Relatively low doping HgCdTe technology,[4] as well as advanced processing and bonding procedures, have led to exceedingly good dark currents well below the target dark current over a large percentage of the array. This represents a real breakthrough in performance over that reported in 2002.

Further author information:
E-mail: candice@astro.pas.rochester.edu

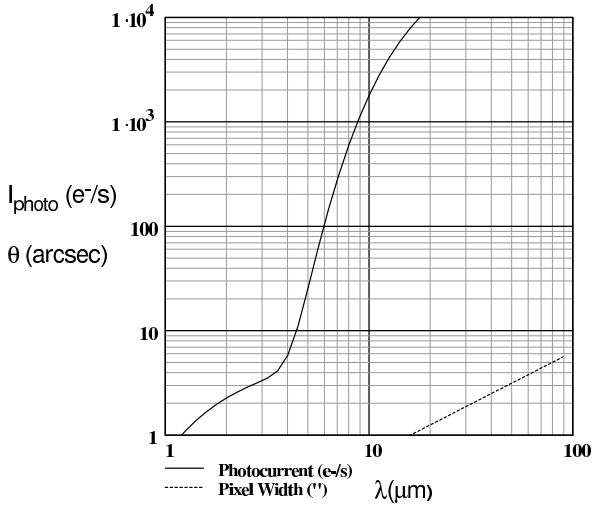

Figure 1. Zodiacal Light emission levels for diffraction limited pixels, QE = 70%, optical efficiency 48%, and spectral resolution $R = 3$. The diffraction-limited pixel width (here $1.22\lambda/D$) is shown for a D = 4m telescope.

2. DATA ACQUISITION AND REDUCTION

The Hawaii-1RG multiplexer is a 1024×1024 pixel read-out integrated circuit (ROIC), with four rows and columns of reference pixels around the perimeter. This leads to 1016×1016 active pixels. It has a selectable number of outputs, plus numerous other features. The Hawaii-1RG is identical in all features and functions to the Hawaii-2RG (see Loose et al. 2003)[5] except for the pixel format (1024×1024 vs. 2048×2048) and number of outputs (1, 2, 16 vs. 1, 4, 32). The Hawaii-1RG was operated in two-output "normal read-out mode" with 100 kHz pixel read rate.

While the Hawaii-1RG has an 18μm pixel pitch designed for SWIR and MWIR HgCdTe, we desire a 36μm pixel pitch for LWIR HgCdTe. Thus the LWIR HgCdTe detector array was bonded to every other pixel of the Hawaii-1RG, resulting in an effective array size of 512×512 (508×508 active) pixels. While this first device does not utilize microlenses despite the much smaller diode size than the pixel pitch (36μm), we plan to implement microlenses in future deliveries to optimize quantum efficiency and fill factor.

Fowler sampling[6] was employed to obtain multiply sampled images for dark current measurements. Other measurements where photon shot noise dominates, such as the capacitance measurement (see Section 2.3), were taken with a single Fowler sample pair, which is equivalent to correlated double sampling. All of the measurements were taken at 0mV applied bias (50mV actual reverse bias, see Section 2.2) and at a temperature of 30K. Due to a short in our electronics that restricted the applied bias to 0mV, we are reporting data with an actual bias very close to zero here. However, it has been shown by Rockwell Scientific Company that applied biases as large as 250mV can be applied without degradation in performance.

2.1. Source Follower Gain

To measure the source follower gain, the reset voltage was varied and the output voltage (Vout) was measured. Then a plot of reset voltage vs. Vout was created and a line fit to the linear portion of the resulting graph. By this method, the source follower gain of the ROIC was measured to be 0.95, as can be seen in Figure 2. The measured gain is the product of the gain of the source follower FET per detector (SFD) and the source follower output FET.

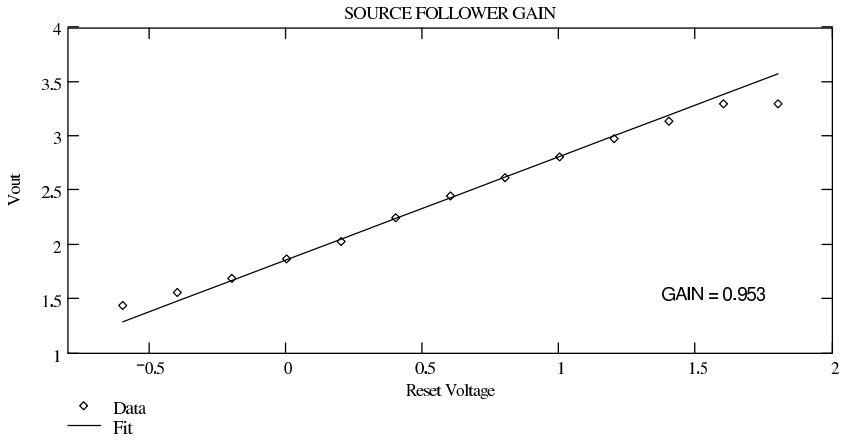

Figure 2. Measurement of the source follower multiplexer gain.

2.2. Well Depth

The well depth is a measure of the amount of charge a pixel can hold. At the beginning of the integration ramp, the bias across a pixel is at its maximum. As the detector integrates, photo-illumination in addition to dark charge deplete the bias. When a pixel is saturated, the actual bias across the pixel is 0mV, so the amount of charge it takes to completely debias the pixel is known as its well depth. The applied bias that corresponds to 0mV well depth is known as the zero bias point (ZBP).

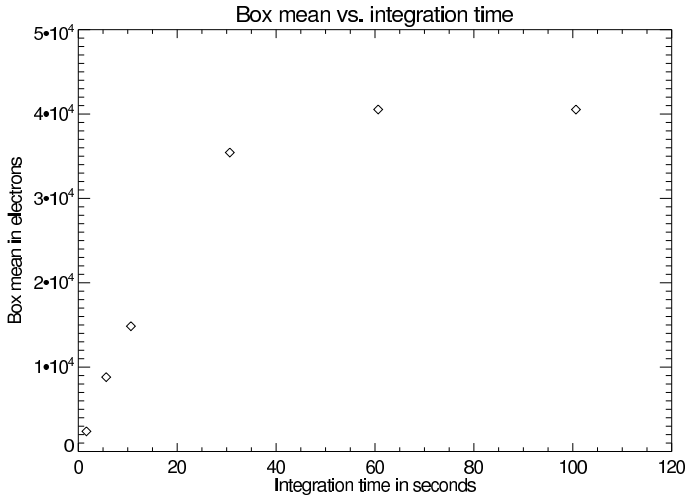

Figure 3. This graph shows the mean signal in electrons of a 20×20 box as a function of integration time in seconds.

The well depth was determined by illuminating the array using a cold K-band filter ($\lambda = 2.2\mu$m) and room illumination. The K-band filter was used in order to achieve a flux low enough for saturation to occur in approximately 60 seconds. This also ensures that the pedestal level has a minimal amount of photo-charge, and minimizes the amount of forward bias when saturation is approached. Data sets with integration times of up to 100 seconds were taken and the saturation level found to be 40,000 electrons (see Figure 3). This implies the back-bias at the start of integration was approximately 50mV (hence ZBP = -50mV).

2.3. Capacitance

Capacitance measurements (Noise^2 vs. Signal) were obtained with a cold K-band (2.2μm) filter and room illumination, with 40 samples per integration time. Data were examined in 20×20 boxes, and the slope of a straight line fit to the Noise^2 vs. Signal data so obtained yielded measures of the e^-/ADU and hence capacitance[7] in the boxes selected from the uniformly illuminated (unvignetted) portion of the images. Interactive Data Language (IDL) was used in reduction to exclude outlier data points. The average capacitance was measured to be 128fF with a standard deviation of 7fF. This corresponds to an average conversion factor of 8.6 e^-/ADU which was used in subsequent calculations. This value is taken from the average of fourteen sample boxes. One representative graph of the capacitance measurement is shown in Figure 4. This is a lower limit to the e^-/ADU and an upper limit on the capacitance because of the possibility of gain in the detector at these wavelengths.

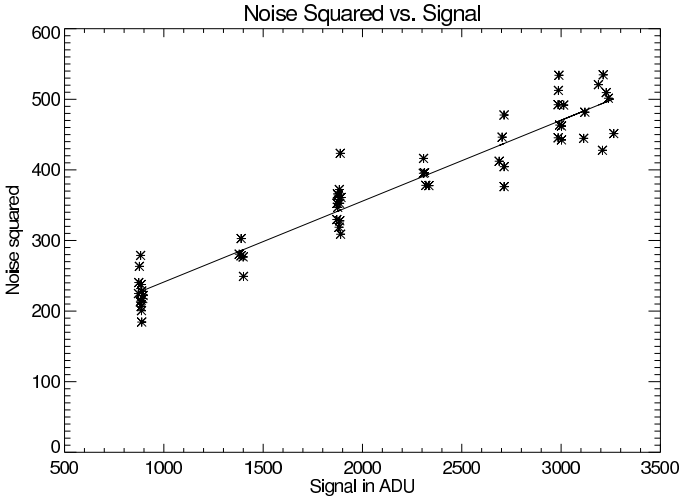

Figure 4. This graph is for a 20×20 box on the array. The slope of this line corresponds to a capacitance of 130fF.

3. TESTING AND RESULTS

3.1. Dark Current Measurements

Dark current frames at a variety of integration times were obtained in a cooled, blackened environment with external light blocked by a liquid helium cooled, blackened plate. A black paper baffle was placed around the detector and prevented off-axis light sources from contributing to the overall signal. Data reduction was done with IDL, and reference pixel corrections were employed in analysis of these measurements. Approximately 5.22% of detector pixels were deemed non-responsive to light. These pixels and the reference pixels were excluded from the results.

Figure 5 shows the dark current distribution for 82.46% of all detector pixels. The remainder of pixels not plotted continue the high-end tail of the distribution. Remarkably, 99.23% of all connected pixels display dark currents less than our goal of $30e^-$/s. This is in contrast to the 30% with dark currents less than $100e^-$/s reported on our earlier devices. It is also apparent that the majority of pixels display dark currents nearly three orders of magnitude less than our goal of $30e^-$/s.

The majority of pixels displayed dark currents between $-0.03e^-$/s and $0.05e^-$/s. This encompassed 51.33% of all detector pixels in the array. The negative values here reflect uncertainty in the measurement. The percentage of pixels with dark currents below $-0.03e^-$/s is 5.26%, where some of these may be slightly forward-biased diodes. The vast majority of pixels with dark currents greater than $0.05e^-$/s still exhibit dark currents less than our goal. Twenty percent of pixels are greater than $0.05e^-$/s and still less than $1e^-$/s. The percentage of pixels greater than $1e^-$/s and less than $30e^-$/s is 17.38%.

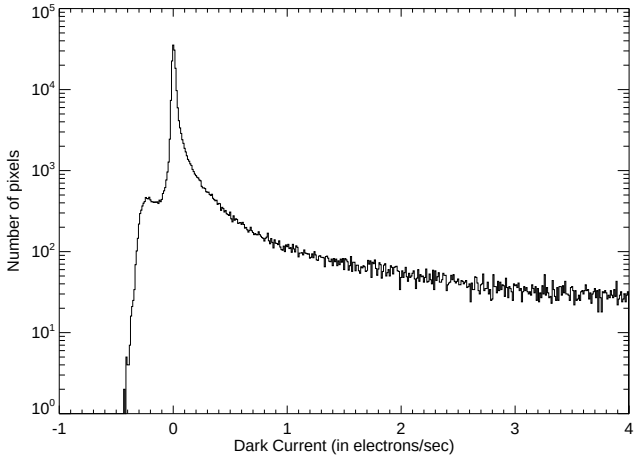

Figure 5. This figure shows the dark current distribution between -1 and $4e^-$/s.

Figure 6 gives a histogram of all detector pixels with dark currents between $-0.04e^-$/s and $0.06e^-$/s. Approximately 53.4% of detector pixels are plotted in this graph. The Gaussian fit has a mean dark current of $0.007e^-$/s and $\sigma = 0.012e^-$/s.

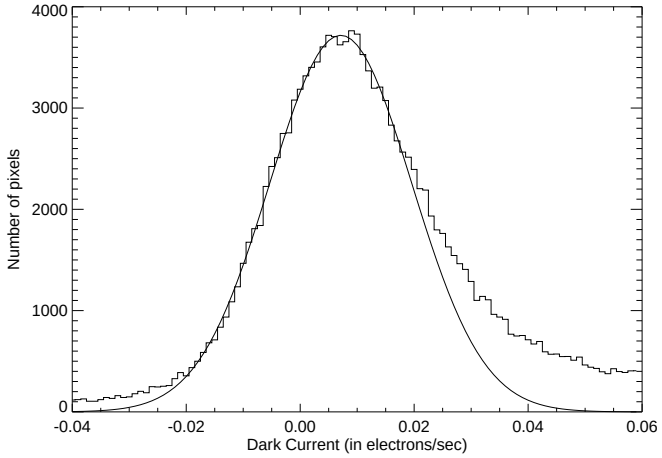

Figure 6. This figure shows the dark current distribution between $-0.04e^-$/s and $0.06e^-$/s.

3.2. Dark Current Uniformity

The dark current is very uniform on this array. Figure 7 is an image which shows the dark current of each pixel in that pixel's location on the array. The scale bar on the right goes from $0e^-$/s to $3e^-$/s. Only 13% of pixels are greater than the upper limit shown here, which is still a full order of magnitude less than our goal. Histograms of this image can be seen in Figure 5 and Figure 6. These histograms show the dark current distribution and emphasize the large number of pixels with very low dark currents. Our ambitious goal of $< 30e^-$/s at a focal plane temperature of T $\sim$ 30K was achieved and significantly surpassed by a large fraction of pixels, showing that uniform, really low dark current arrays are becoming possible.

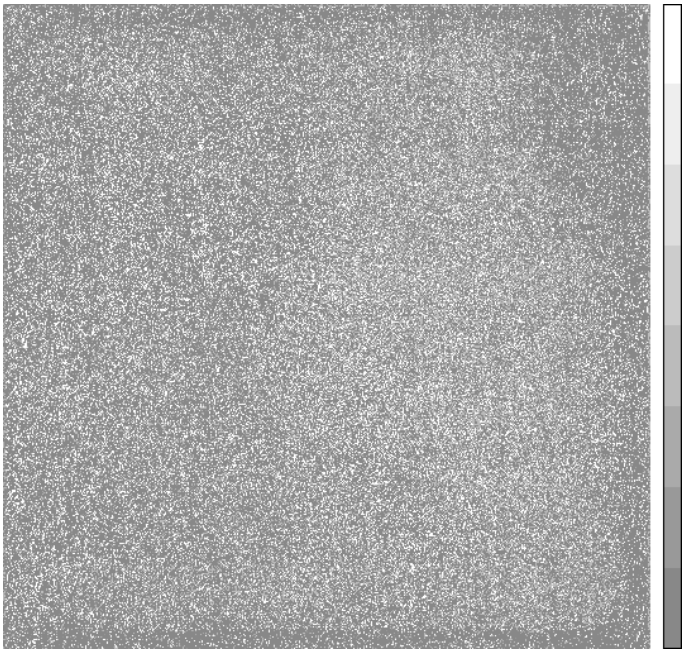

Figure 7. This image shows dark currents from 0 to $3e^-$/s.

3.3. Relative Response and Cutoff Wavelength

The cutoff wavelength for the array was determined by illuminating the array with room-temperature radiation through a long-wave circular variable filter wheel and measuring the half power point of the relative detector response. The dependence of this response on wavelength can be seen in Figure 8. The cutoff wavelength shown is 9.6μm.

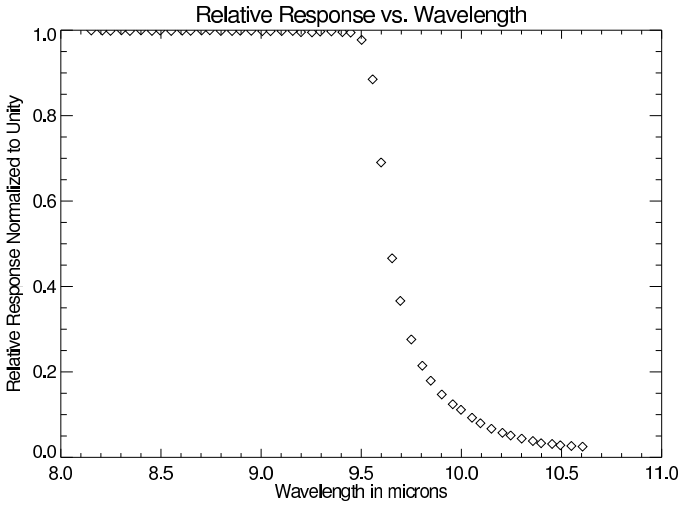

Figure 8. Relative Response of the Detector vs. Wavelength

4. CONCLUSIONS

Results presented here are very preliminary, and only encompass one week of testing following delivery. However, results presented on this first device represent a breakthrough in materials processing over ultralow background application LWIR HgCdTe arrays we have tested at Rochester in the past. The mean dark current of the Gaussian fit to this array's dark current distribution is $0.007e^-$/s, with $\sigma = 0.012e^-$/s. This encompasses over half of the pixels on the array. Over 99% of all working detector pixels have dark currents under our goal of $30e^-$/s.

It is clear that Rockwell Scientific Company has produced uniform, remarkably low dark current HgCdTe LWIR arrays, suitable for ultralow backgrounds in space astronomy. Choices among diode geometries have been made from prior experiments, and processing and architectures have been vastly improved in the last year. This device, being the first delivery with the new processing techniques, has shown exceptional performance and operability. Remaining tasks include addition of microlenses to improve pixel QE and fill factor, and extension of the techniques to longer wavelengths. We are now extremely optimistic that space quality devices useful to low background astronomy can and will be made.

ACKNOWLEDGMENTS

We are grateful for support for this program. Specifically we acknowledge NASA grants NAG5-6267 and NAG5-8642, as well as NASA Ames grant NAG2-1533.

REFERENCES

1. A. D. Estrada, G. Domingo, J. D. Garnett, A. W. Hoffman, N. A. Lum, P. J. Love, S. L. Solomon, J. E. Venzon, G. R. Chapman, K. P. Sparkman, C. R. McCreight, M. E. McKelvey, R. E. McMurray, J. A. Estrada, S. Zins, R. McHugh, and R. Johnson, "Si:As IBC IR focal plane arrays for ground-based and space-based astronomy," in *Proc. SPIE Vol. 3354, p. 99-108, Infrared Astronomical Instrumentation, Albert M. Fowler; Ed.*, **3354**, pp. 99–108, Aug. 1998.
2. C. Bacon, J. L. Pipher, W. J. Forrest, C. W. McMurtry, and J. D. Garnett, "Diode Characterization of Rockwell LWIR HgCdTe Detector Arrays," in *IR Space Telescopes and Instruments. Edited by John C. Mather. Proceedings of the SPIE, Volume 4850, pp. 927-934 (2003).*, pp. 927–934, Mar. 2003.
3. R. B. Bailey, J. M. Arias, W. V. McLevige, J. G. Pasko, A. C. Chen, C. Cabelli, L. J. Kozlowski, K. Vural, J. Wu, W. J. Forrest, and J. L. Pipher, "Prospects for large-format IR astronomy FPAs using MBE-grown HgCdTe detectors with cutoff wavelength $> 4\mu$m," in *Proc. SPIE Vol. 3354, p. 77-86, Infrared Astronomical Instrumentation, Albert M. Fowler; Ed.*, **3354**, pp. 77–86, Aug. 1998.
4. J. Wu, *Development of Infrared Detectors for Space Astronomy, PhD Thesis*, University of Rochester, Rochester, NY, 1997.
5. M. Loose, M. C. Farris, J. D. Garnett, D. N. B. Hall, and L. J. Kozlowski, "HAWAII-2RG: a 2k x 2k CMOS multiplexer for low and high background astronomy applications," in *IR Space Telescopes and Instruments. Edited by John C. Mather . Proceedings of the SPIE, Volume 4850, pp. 867-879 (2003).*, pp. 867–879, Mar. 2003.
6. A. M. Fowler and I. Gatley, "Noise reduction strategy for hybrid IR focal-plane arrays," in *Proc. SPIE, Infrared Sensors: Detectors, Electronics, and Signal Processing*, T. S. Jayadev, ed., **1541**, pp. 127–133, Nov. 1991.
7. L. Mortara and A. Fowler, "Evaluations of CCD: Performance for Astronomical Use," *Proc. SPIE, Solid State Imagers for Astronomy* **290**, pp. 28–30, 1981.